

# Resilience of LTE-A/5G-NR links Against Transient Electromagnetic Interference

Sharzeel Saleem

*Department of Electrical and Electronic Engineering  
University of Bristol  
Bristol, United Kingdom  
Sharzeel.saleem@gmail.com*

Mir Lodro

*Department of Electrical and Electronic Engineering  
University of Bristol  
Bristol, United Kingdom  
mir.lodro@bristol.ac.uk*

**Abstract**—This paper presents a comparative analysis of long-term evolution advanced (LTE-A) and fifth-generation new radio (5G-NR), focusing on the effects of Transient Electromagnetic Interference (EMI) caused by catenary-pantograph contact in a railway environment. We developed a software-defined radio (SDR)-based prototype for the performance evaluation of LTE-A and 5G-NR links in the presence of transient interference. The results show that both links experience considerable degradation due to interference at different center frequencies. Performance degradation is proportional to the gain of interference. The measurement results show that both links experience considerable performance degradation in the presence of transient EM interference.

**Index Terms**—5G-NR, 3GPP, LTE-A, Transient EMI, Catenary-Pantograph.

## I. INTRODUCTION

Wireless systems such as 5G-NR and LTE-A operate in complex propagation environments and are susceptible to electromagnetic interference. Electromagnetic interference, such as transients generated by high-power generators or emissions from loose pantograph-catenary systems, degrades the performance of wireless systems [1] [2]. Transient electromagnetic interference can cover a wide range of the spectrum, including the WiFi and cellular bands. Hence, electromagnetic interference can affect both the primary user link from the eNB/gNB to the user equipment (UE) onboard and on the platform. It can also affect the performance of secondary wireless links, such as WiFi AP, to onboard users. It can also introduce additional problems in spectrum-sharing scenarios where primary and secondary user networks coexist and use energy detection to detect the presence of primary users. Transient EMI sources are difficult to locate. Furthermore, transient EMI can appear random and inconsistent, depending on the physical state of the fault location. The intermittent contact between the catenary and pantograph generates a wideband signal capable of jamming communication links across a broad range of frequencies. This paper aims to investigate the effects of unintentional interference on the communication link. The key performance indicators used to measure these effects are error vector magnitude (EVM), bit error rate (BER), and signal-to-interference plus noise ratio (SINR). We have divided our work into five sections. Section I is the introduction. In Section II, we discuss the background of the problem and highlight

the latest contributions. In Section III, we introduce the setup of the experiment and our methodology and explain key performance indicators. Section IV is about the measurement results and the effect of transient interference on LTE-A and 5G-NR. The conclusion of the study is given in Section V.

## II. LITERATURE SURVEY

Transient electromagnetic interference papers focus on evaluating the performance of communication links with some key performance indicators (KPIs) assessment. The authors in [3], have provided a comprehensive overview of the impact of intentional and unintentional sources of EMI on the global system for mobile communication (GSM), LTE-R, and 5G-R. They have detailed the sources of EMI not only from pantograph arcing but also from various other sources of intentional and unintentional EMIs. They have explained the impact of interference coming from onboard power electronics and narrowband jammers. Their measurement results suggest a degrading impact on system performance, particularly concerning bit error rates as the interference power increases. The work in [4], presents a real-time classification method for EMI and intentional EMI. The authors have provided a brief overview of transient and sweep interference. They have used machine learning to check the classification accuracy of different sources of interference at a center frequency of 1.9 GHz and different channel parameters. The works in [5] and [6] focus on the evaluation of intentional and unintentional interferences found in the transportation sector, particularly used in high-speed train scenarios. They have particularly focused on the interference effect on the IEEE 802.11n WiFi hotspot onboard trains. The IEEE 802.11n standard operates in the 2.4-GHz and 5-GHz bands with different modulation and bandwidth requirements. The authors in the paper [7], have also evaluated the influence of pantograph arcing on the LTE-R. With the help of simulation, they show the impact of arcing on the block error rate and LTE throughput. The study concludes with evidence of system performance degradation. Similarly, the authors in [8] have shown a transient impact of EMI on LTE communication. They have considered EVM and peak-to-average power ratio (PAPR) as the main KPIs for performance evaluation. They have provided a detailed account of the LTE PHY layer and have shown the impact of

EMI on EVM and PAPR as the interference-to-signal power ratio increases. The work [9], has evaluated the impact of pantograph-catenary transient emission on the performance of the IEEE 802.11n standard in the entire 2.4-2.5-GHz band. They have performed detailed bit error measurements with different time interval durations. They have found that the bit error gets worse as the duration of the transient interference increases. The work presented by [10] includes a detailed study of the impact of pantograph-catenary emission on railway communications. They have focused on the evaluation of the deployment of antenna systems for GSM-R and LTE-R at frequencies of 380, 900, 2600, and 5900 MHz respectively. The research presented by [11] examines electromagnetic disturbances caused by loose catenary-pantograph contact. The experiment demonstrated that when the pantograph-catenary spacing remains constant, increasing the voltage level leads to a higher current in the discharge circuit, which intensifies impulse radiation during contact loss events. Long-Term Evolution-Metro (LTE-M) is a dedicated communication system for train control, with stringent requirements regarding adjacent channel interference (ACI). The research in [12] proposes a solution using the Monte Carlo method to analyze the convergence of different scenarios where LTE-M and ACI coexist.

### III. METHODOLOGY

This experiment aimed to assess the impact of Transient Electromagnetic Interference (EMI) on a controlled communication link created using commercial off-the-shelf (COTS) software-defined radio from National Instruments. We used NI universal software radio peripheral (USRP)-2943R equivalent to Ettus Research X310 USRP. We used a CBX-40 RF card with NI USRP-2943R which can provide a full-duplex bandwidth of 40 MHz. Our experimental setup includes three NI USRPs equipped with CBX-40 RF cards. We used two separate NI USRPs to create the main communication link. The main communication link is created by transmitting and receiving standardized LTE and 5G-NR waveforms and obtaining repeatable BER and EVM performance. We used LTE Toolbox and 5G Toolbox to generate and process standardized waveforms. We used MATLAB Wireless Testbench to transmit and receive high-speed complex waveforms without dropped samples. The third NI USRP with similar RF and digital specifications was used to generate RF interference signals at different center frequencies. The setup involved three USRPs and an R&S Spectrum analyzer for monitoring the PSD of the received signal in the presence of interference. Frequency scanning between 2.194 and 2.2045 GHz identified the center frequencies most vulnerable to EMI, with gains adjusted to 12 dB, 15 dB, and 18 dB. The findings highlighted a significant impact at 18 dB gain, which effectively disrupted communication, underscoring the potential severity of transient EMI at higher interference gains. This effect of the 18 dB gain on signal degradation is discussed in detail in this paper, revealing critical insights into EMI resilience and vulnerability in different frequencies and gain settings.

#### A. Types of Unintentional Interferences

Unintentional interference such as transient interference can come from different sources. In the railway environment, unintentional transient interference is produced by high-power generators and the arcing effect of pantograph-catenary contact. Unintentional interference can arise from numerous sources, such as switching of power supplies or operation of high-power motors. A notable example is the electromagnetic interference produced when pantographs on trains come into contact with catenary wires, as shown in Fig. 1.



Fig. 1. Catenary-Pantograph Contact.



Fig. 2. Road transport powered by electricity [13].

In current times, innovations in power supply systems for road transport have aimed to reduce emissions but also introduce potential sources of transient electromagnetic interference. As shown in Figure 2, the movement of vehicles on highways equipped with these systems can inadvertently interfere with communication links. The effect can be severe if tram overhead lines pass through the city center or critical infrastructure that can disrupt communication links such as long-range (LoRA), WiFi, and LTE-A. Another source of unintentional interference is the SPN-43 radar, which operates in the S-band for the location of military targets, which can disrupt nearby communication systems. Furthermore, dynamic

TABLE I  
LTE-A PHY COMMUNICATION LINK PARAMETERS

Parameter	Value
Base RMC Configuration	R.7 (10 MHz)
Jammer Sampling Rate	15.36 MHz
Power Scale Factor	0.8
Jammer Radio Gain	2 dB
eNodeB (TX) Radio Gain	25 dB
UE (RX) Radio Gain	20 dB
Center Frequency	2.2 GHz
EVM Peak	17.771%
EVM RMS	5.049%
BER	0
Frequency Offset	1372.998 Hz

spectrum sharing (DSS) in the citizens broadband radio service (CBRS) spectrum improves spectrum efficiency, but can also introduce interference between shared bands, challenging communication reliability [14].

### B. Testbed Configuration and Parameter Specifications

The experimental setup facilitates a thorough analysis of how various interference parameters affect the stability and performance of the communication link. In the context of an LTE-A/5G-NR communication link, a series of experiments were carried out. The PHY layer parameters of the LTE-A and 5G-NR as shown in Tables I and II respectively. For the transmission and reception of the baseband waveforms, we used separate USRPs to rule out the effect of cross-channel leakage. Fig. 3 shows the photo of the experimental setup where three X310 USRPs are connected to the Intel Core i7 laptop via an Ethernet switch. We generate transient electromagnetic interference at various RF frequencies within the bandwidth of interest. The initial phase included frequency scanning to pinpoint the frequencies most susceptible to performance degradation under jamming conditions. The findings revealed that the center frequencies of 2.1955 GHz, 2.2 GHz, and 2.2045 GHz were especially vulnerable to interference.

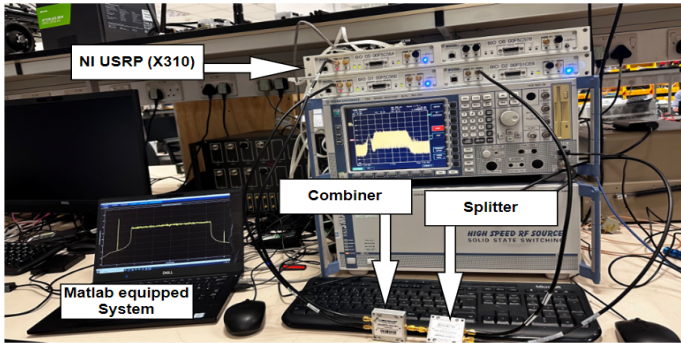


Fig. 3. Photo of the experimental setup.

The bandwidth used in this experiment is 10 MHz. Additionally, the EVM is worse as the interference increases, particularly for higher-order modulation such as 64-QAM. In the absence of interference, it was observed that the EVM RMS is approximately 5%, which is as low as possible with

TABLE II  
5G-NR COMMUNICATION LINK PARAMETERS

Parameter	Value
Frequency Range	410 MHz - 7.125 GHz
Modulation Coding Scheme	64-QAM, R=3/4
Channel Bandwidth	10 MHz
Sampling Rate	15.36 MHz
TX Radio Gain	20 dB
RX Radio Gain	20 dB
Jammer Radio Gain	2 dB
Center Frequency	2.2 GHz
Subcarrier Spacing	30 kHz

a zero bit error rate. The generated waveform uses 64-QAM modulation with a Forward Error Correction (FEC) code rate of 3/4. With a sub-carrier spacing of 30 kHz and a bandwidth of 10 MHz, it supports up to 24 resource blocks.

### C. Transient Electromagnetic Interference (EMI)-Unintentional Interference

The interaction between the catenary and pantograph generates transient broadband electromagnetic waves. Numerous studies have been conducted on the characterization of these fast-radiated transient disturbances resulting from the sliding contact of the pantograph on the catenary. These studies utilize various approaches, including a spectral approach, as discussed in article [15], a temporal approach, as explored in article [16], and a combination of both approaches, as examined in articles [17] and [18]. The setup utilizes a double-sided transient waveform to investigate the effects on the LTE communication link. Mathematically, the wave can be written as the double-sided transient waveform is given by:

$$s_{\text{trans}}(t) = A_0 \left( e^{-\frac{t}{\tau_{\text{rise}}}} - e^{-\frac{t}{\tau_{\text{hold}}}} \right) \sin(2\pi f_c t) \cdot u(t) \quad (1)$$

where:  $A_0$  is the amplitude,  $f_c$  is the carrier frequency, and  $u(t)$  is the unit step function,  $\tau_{\text{rise}}$  is the rise time constant, can be in the range of 0.1 and 3ns but taken as 2ns for this experiment,  $\tau_{\text{hold}}$  is the hold time constant, can be in the range of 1ns and 50ns but taken as 30ns for this experiment.

### D. Key Performance Indicators

The primary key performance Indicators(KPIs) are Error Vector Magnitude (EVM) and Signal-to-Interference-plus-Noise Ratio (SINR).

1) *Error Vector Magnitude (EVM)*: EVM is defined as the measure of how far the actual transmitted signal deviates from the ideal or reference signal in a constellation diagram. In simpler terms, it measures the difference between the ideal signal points and the points where the actual received signal ends up due to various imperfections in the transmission process [19]. The equation for calculating EVM is given by:

$$\text{EVM} (\%) = \frac{\sqrt{\frac{1}{N} \sum_{i=1}^N |S_{\text{ref}}[i] - S_{\text{received}}[i]|^2}}{\sqrt{\frac{1}{N} \sum_{i=1}^N |S_{\text{ref}}[i]|^2}} \times 100 \quad (2)$$

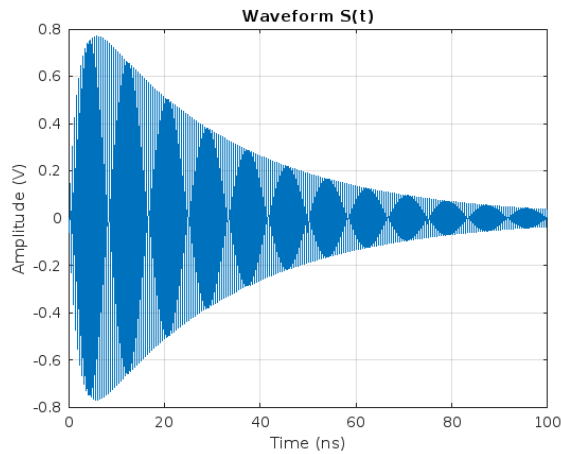


Fig. 4. Double-sided exponential wave at 2.2 GHz.

where:  $S_{\text{ref}}[i]$  is the ideal symbol or the reference symbol at the  $i$ -th symbol and  $S_{\text{received}}[i]$  is the  $i$ -th received symbol.  $N$  is the total number of complex symbols.

2) *Signal-to-Interference-plus-Noise Ratio (SINR)*: SINR evaluates the quality of the radio link between a base station and the user equipment (UE). It is a ratio of the power of the intended received signal  $P_{\text{signal}}$  to the power of the interference signal  $P_{\text{interference}}$  plus noise power  $P_{\text{noise}}$

$$\text{SINR} = \frac{P_{\text{signal}}}{P_{\text{interference}} + P_{\text{noise}}} \quad (3)$$

For the OFDM-specific waveforms, the SINR at subcarrier  $k$  is:

$$\text{SINR}_k = \frac{|H_k|^2 P_{\text{Tx}}}{\sum_{j \neq k} |I_j|^2 P_{\text{Tx}} + N_0 B_k} \quad (4)$$

where  $H_k$  is the channel frequency response for the subcarrier  $k$ .  $P_{\text{Tx}}$  is the power of the signal transmitted per subcarrier.  $|I_j|^2$  is the power of interference.  $N_0$  and  $B_k$  are the spectral density of the noise power and the bandwidth of the subcarrier  $k$ , respectively. We consider the signal power received from the demodulated OFDM symbols. This metric is crucial for network operators, as it helps to assess and optimize network resilience.

#### IV. RESULTS AND DISCUSSIONS

The experimental results are organized into two sections: the first details the impact of a double-sided exponential jammer (Transient EMI) on an LTE-A link, while the second examines its effect on a 5G-NR link. Finally, a comparison is performed to determine which communication link is more susceptible to this type of interference.

##### A. Transient EMI in LTE-A

A double-sided exponential jammer with adjustable gain and varying center frequencies was tested. At a transmit gain of 18 dB, the impact was substantial, with key performance indicators (KPIs) summarized in the table below III. We can see the impact of transient interference. The BER of the

TABLE III  
KPI MEASUREMENTS OF 5G-NR LINK AT DIFFERENT RF FREQUENCIES IN THE PRESENCE OF TRANSIENT INTERFERENCE. THE GAIN OF THE INTERFERING USRP IS SET TO 18 dB.

Interferer Frequency	EVM Peak	EVM RMS	BER	Frequency Offset(Hz)	SINR (dB)
2.1955 GHz	829.12%	79.212%	0.24165	1680.86	1.89
2.2 GHz	1985.256%	85.549%	0.32059	2132.578	4.5046
2.2045 GHz	1387.908%	83.565%	0.26159	2082.8	-0.2355

communication link at all the selected frequencies is very high. We also presented the frequency offset, peak EVM, and RMS EVM at all interference center frequencies. The peak RMS EVM is worst when the interference RF frequency is 2.2 GHz.

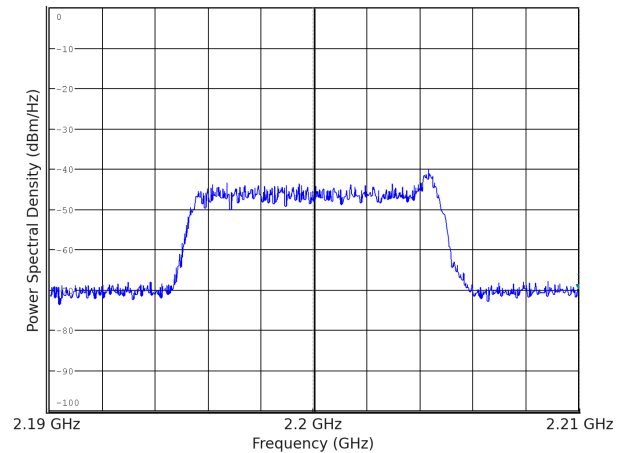


Fig. 5. Power Spectral Density due EMI at 2.2045 GHz.

The experimental results indicate a significant degradation in the Signal-to-Interference-plus-Noise Ratio (SINR), which decreased from 15.1226 dB to -0.23355 dB. This drop represents the maximum performance degradation observed in the LTE communication link, despite employing a high transmit gain intended to mitigate such losses.

Figure 5 illustrates a peak centered at 2.2045 GHz, resulting from the injection of transient electromagnetic interference (EMI). This EMI not only contributes to the SINR reduction, but also leads to substantial distortion in the signal constellation. As shown in Figure 8, the constellation exhibits the effect of noise that can vary between symbols. This noise around the ideal symbol configuration suggests that the received symbols are displaced from their intended positions, reflecting the detrimental effects of frequency distortion on the integrity of the signal and the overall performance of the LTE communication system. Additionally, the received constellation appears to be a single noise cloud around the origin if the magnitude of the interference increases to a level where the decodability of the data symbols is not possible. These findings underscore the critical impact of transient EMI on the reliability of LTE communications.

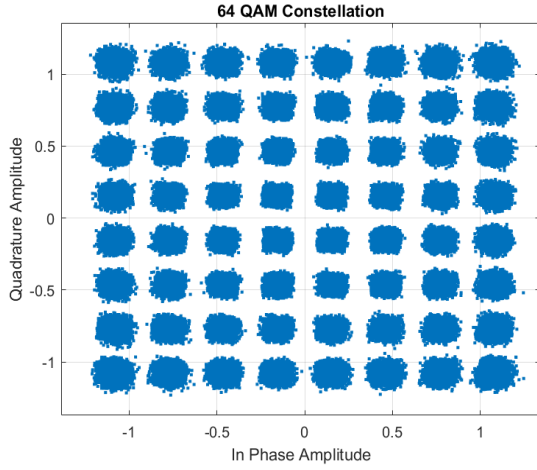


Fig. 6. Received 64-QAM constellation.

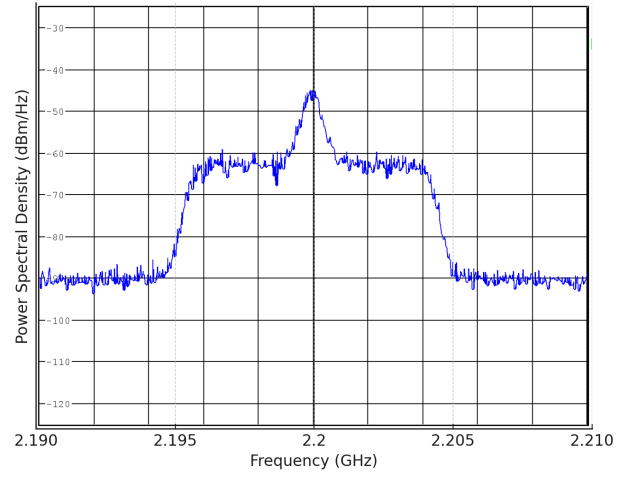


Fig. 7. Power Spectral Density due EMI at 2.2 GHz.

TABLE IV

KPI MEASUREMENTS OF 5G-NR LINK AT DIFFERENT RF FREQUENCIES IN THE PRESENCE OF TRANSIENT INTERFERENCE. THE GAIN OF THE INTERFERING USRP IS SET TO 18 dB.

Interferer Frequency	EVM Peak	EVM RMS	BER	SINR (dB)
2.1955 GHz	389223.16%	3201.15%	0.3214	3.52
2.2 GHz	107336.92%	1774.27%	0.3884	-12.67
2.2045 GHz	285892.70%	2446.83%	0.3503	-3.64

### B. Transient EMI in 5G-NR

A double-sided exponential signal was introduced into the primary communication link at three distinct transmit gains, mirroring the configuration used in the LTE link. All parameters were kept constant, except for the operating frequency. As indicated in the table, the signal at 2.2 GHz shows the greatest performance degradation, although its impact is still less severe compared to that of the continuous wave (CW) tone jammer.

A pronounced peak is evident in Figure 7, attributed to the jammer effect. This peak signifies a notable increase in energy, subsequently leading to distortion in the Error Vector Magnitude (EVM) resource grid depicted in Figure 9. This phenomenon is observed when the jammer transmit gain is configured to 18 dB. The presence of the jammer introduces significant interference into the communication link, contributing to a higher EVM peak.

The high EVM values indicate a degradation in signal quality, reflecting the extent of distortion caused by the interference signal. As the interference gain increases, the interference becomes more pronounced, negatively affecting the integrity of the transmitted signal. This scenario highlights the critical impact of jamming on communication systems, particularly in environments where the signal-to-noise ratio is already compromised. The distortion in the EVM resource grid further illustrates the challenges in maintaining reliable communication under such adverse conditions, underscoring the necessity for robust interference mitigation strategies in

TABLE V

FINAL MEASUREMENT RESULTS OF LTE-A AND 5G-NR COMMUNICATION LINKS WITHOUT AND WITH INTERFERENCE.

Interferer Type	EVM Peak (%)	BER (%)	SINR (dB)
LTE-A Link	17.77	0.00	15.12
5G-NR Link	23.76	0.00	15.97
LTE Transient EM Wave Jammer @ 2.2045 GHz, 18 dB Gain	1387.91	0.26	-0.20
5G-NR Transient EM Wave Jammer @ 2.2 GHz, 18 dB Gain	107336.97	0.39	-12.67

practical implementations.

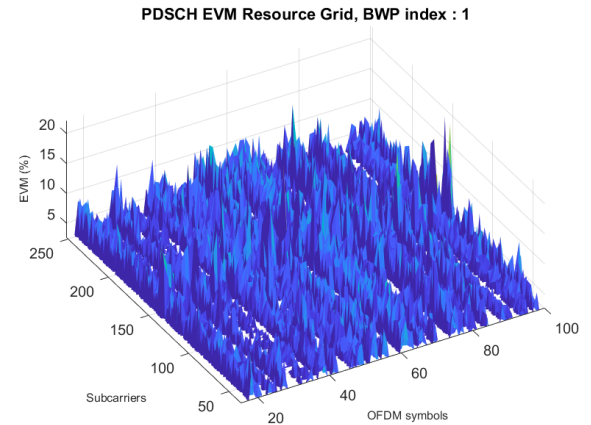


Fig. 8. EVM resource grid without interference.

The final EVM and BER evaluation of both communication links is summarized in Table. V. It can be observed that the BER and EVM in both communication links are high when there is interference at the center frequency of 2.2045 GHz at an interference gain value of 18 dB.

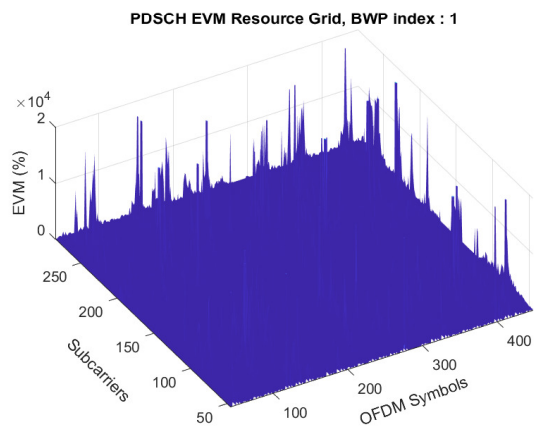


Fig. 9. EVM resource grid @ 2.2 GHz under interference.

## V. CONCLUSION AND FUTURE SCOPE

We conducted an experimental evaluation of the susceptibility of the communication links using software-defined radio platforms. The measurement results indicate that the 5G-NR link experiences a greater degradation in capacity and bit error rate (BER) when subjected to unintentional interference. Previous reports have highlighted disruptions in communication links near hospitals and universities where tram routes are present. The experimental findings support the claim that LTE systems demonstrate greater resilience to high-frequency interference. Therefore, it is essential to implement measures to mitigate these effects and improve the reliability of communication systems in vulnerable areas. The future direction of this research aims to build on the findings of the current experiments by conducting a more detailed investigation of the specific locations and causes of interference affecting communication systems. This will involve a comprehensive analysis of environmental factors, infrastructure layouts, and potential sources of unintentional electromagnetic interference.

## REFERENCES

- [1] A. N. de São José, N. Chopinet, E. P. Simon, V. Deniau, and N. Beuwe, "Contribution to a harmonized test methodology to compare railway wireless communication technologies under transient interference," *IEEE Transactions on Electromagnetic Compatibility*, 2023.
- [2] A. N. de São José, N. Chopinet, V. Deniau, and E. P. Simon, "Designing a sequence of transient em signals in order to test railway wireless communications face to em interferences produced by the catenary-pantograph contact," in *2023 International Symposium on Electromagnetic Compatibility-EMC Europe*. IEEE, 2023, pp. 1–6.
- [3] Y. Fan, L. Zhang, and K. Li, "Emi and iemi impacts on the radio communication network of electrified railway systems: A critical review," *IEEE Transactions on Vehicular Technology*, vol. 72, no. 8, pp. 10 409–10 424, 2023.
- [4] Y. Fan, L. Zhang, K. Li, M. Bao, and M. Lu, "Deep learning-based emi and iemi classification in 5g-r high-speed rail wireless communications," in *2024 IEEE 99th Vehicular Technology Conference (VTC2024-Spring)*. IEEE, 2024, pp. 1–6.
- [5] G. Romero, "Identification of the impact mechanisms of the electromagnetic interferences on the wi-fi communications," Ph.D. dissertation, UNIVERSITÉ DE LILLE 1 SCIENCES ET TECHNOLOGIES, 2017.

- [6] V. Deniau, C. Gransart, G. L. Romero, E. P. Simon, and J. Farah, "Ieee 802.11 n communications in the presence of frequency-sweeping interference signals," *IEEE Transactions on Electromagnetic Compatibility*, vol. 59, no. 5, pp. 1625–1633, 2017.
- [7] J. Wang, G. Wang, D. Zhang, J. Zhang, and Y. Wen, "The influence of pantograph arcing radiation disturbance on lte-r," in *2019 International Conference on Electromagnetics in Advanced Applications (ICEAA)*. IEEE, 2019, pp. 0583–0586.
- [8] O. Stienne, V. Deniau, and E. P. Simon, "Assessment of transient emi impact on lte communications using evm & papr," *IEEE Access*, vol. 8, pp. 227 304–227 312, 2020.
- [9] G. Romero, E. P. Simon, V. Deniau, C. Gransart, and M. Kousri, "Evaluation of an ieee 802.11 n communication system in presence of transient electromagnetic interferences from the pantograph-catenary contact," in *2017 XXXIInd General Assembly and Scientific Symposium of the International Union of Radio Science (URSI GASS)*. IEEE, 2017, pp. 1–4.
- [10] M. M. Correia, "Analysis of the influence of pantographs in railway communications," 2019.
- [11] Y. Yang, H. Cao, M. Zhang, Z. Su, M. Hu, M. Jin, and S. Liu, "Research on the influence of pantograph catenary contact loss arcs and zero-crossing stage on electromagnetic disturbance in high-speed railway," *Energies*, vol. 17, p. 138, 12 2023.
- [12] H. Fu, X. Wang, X. Zhang, A. Saleem, and G. Zheng, "Analysis of lte-m adjacent channel interference in rail transit," *Sensors*, vol. 22, no. 10, 2022. [Online]. Available: <https://www.mdpi.com/1424-8220/22/10/3876>
- [13] G. Romero, "Identification of the impact mechanisms of the electromagnetic interferences on the wi-fi communications," Ph.D. dissertation, 12 2017.
- [14] Y. Fan, L. Zhang, and K. Li, "Emi and iemi impacts on the radio communication network of electrified railway systems: A critical review," *IEEE Transactions on Vehicular Technology*, vol. 72, no. 8, pp. 10 409–10 424, 2023.
- [15] V. Deniau, N. Ben Slimen, S. Baranowski, H. Ouaddi, J. Rioult, and N. Dubalen, "Characterisation of the em disturbances affecting the safety of the railway communication systems," in *2007 IET Colloquium on Reliability in Electromagnetic Systems*, 2007, pp. 1–5.
- [16] M. Ben Slimen, V. Deniau, J. Rioult, S. Dudoyer, and S. Baranowski, "Statistical characterisation of the em interferences acting on gsm-r antennas fixed above moving trains," *The European Physical Journal Applied Physics*, vol. 48, pp. 1–7, 11 2009.
- [17] Y. Wen, B. Sun, Q. Wang, and Z. Tan, "Research on the emi radiation of discharge of pantograph-offline on emu," in *2014 International Conference on Electromagnetics in Advanced Applications (ICEAA)*, 2014, pp. 562–565.
- [18] C. Song, "Three types of electromagnetic noise between pantograph and catenary," 11 2009, pp. 40 – 43.
- [19] O. Stienne, V. Deniau, and E. P. Simon, "Assessment of transient emi impact on lte communications using evm & papr," *IEEE Access*, vol. 8, pp. 227 304–227 312, 2020.